SGN – Assignment #1

Davide Zamblera, 994071

1 Periodic orbit

Exercise 1

Consider the 3D Sun–Earth Circular Restricted Three-Body Problem with $\mu = 3.0359 \times 10^{-6}$.

1) Find the x-coordinate of the Lagrange point L_2 in the rotating, adimensional reference frame with at least 10-digit accuracy.

Solutions to the 3D CRTBP satisfy the symmetry

$$\mathcal{S} : (x, y, z, \dot{x}, \dot{y}, \dot{z}, t) \rightarrow (x, -y, z, -\dot{x}, \dot{y}, -\dot{z}, -t).$$

Thus, a trajectory that crosses perpendicularly the $y = 0$ plane twice is a periodic orbit.

2) Given the initial guess $\mathbf{x}_0 = (x_0, y_0, z_0, v_{x0}, v_{y0}, v_{z0})$, with

$$\begin{aligned} x_0 &= 1.008296144180133 \\ y_0 &= 0 \\ z_0 &= 0.001214294450297 \\ v_{x0} &= 0 \\ v_{y0} &= 0.010020975499502 \\ v_{z0} &= 0 \end{aligned}$$

Find the periodic halo orbit that passes through z_0; that is, develop the theoretical framework and implement a differential correction scheme that uses the STM either approximated through finite differences or achieved by integrating the variational equation.

The periodic orbits in the CRTBP exist in families. These can be computed by continuing the orbits along one coordinate, e.g., z_0. This is an iterative process in which one component of the state is varied, while the other components are taken from the solution of the previous iteration.

3) By gradually increasing z_0 and using numerical continuation, compute the families of halo orbits until $z_0 = 0.0046$.

(8 points)

The objective of this work is the definition by initial state of a family of Halo orbits in the dynamical environment of the Sun-Earth CRTBP in adimensional units. The CRTBP is a dynamical model where a spacecraft or any secondary object, in terms of mass, is under the influence of two main attractor bodies, in a rotating reference frame. The equations are then derived from Newton's law of motion and a variation of the frame of reference. The equations are expressed in a state-space form and reported in Eq. (1).

In the equation $r_1 = \sqrt{(x+\mu)^2 + y^2 + z^2}$ and $r_2 = \sqrt{(x+\mu-1)^2 + y^2 + z^2}$ are the distances of the spacecraft from the main bodies.

$$\begin{cases} \dot{\boldsymbol{r}} = \boldsymbol{v} \\ \dot{\boldsymbol{v}} = -\boldsymbol{\omega} \times (\boldsymbol{\omega} \times \boldsymbol{r}) - \frac{(1-\mu)}{r_1^3}\boldsymbol{r_1} - \frac{\mu}{r_2^3}\boldsymbol{r_2} - 2\boldsymbol{\omega} \times \boldsymbol{v} \end{cases} \tag{1}$$

Part of the equation which is dependant on r is a composition of conservative forces and can be expressed by the gradient of a potential,$\nabla U = [U_x \; U_y \; U_z]$, in Eq. (2).

$$U = \frac{1}{2}(x^2 + y^2) + \frac{(1-\mu)}{r_1} + \frac{\mu}{r_2} \tag{2a}$$

$$\ddot{x} - 2\dot{y} = U_x, \quad \ddot{y} + 2\dot{x} = U_y, \quad \ddot{z} = U_z \tag{2b}$$

Using this last form and imposing the equilibrium by zeroing all time derivatives we obtain a system of equations that identifies the Lagrange points. For the proposed Halo orbit it is of interest finding the L2 collinear point. This is obtained by imposing y=0 and z=0 and solving Eq. (3) in a range which starts right after the Earth position. The solution was achieved with the bisection method and a 10-digit accuracy, the results are in Table 1

x_{L2}	error f(x)	Search Range
1.0100701875	2.18983E-10	[1.001 1.25]

Table 1: L2 point result

$$U_x = x - \frac{(1-\mu)}{r_1^3}(x+\mu) - \frac{\mu}{r_2^3}(x+\mu-1) = 0 \tag{3}$$

An Halo orbit is a periodic orbit which can be achieved in the vicinity of a libration point, a first order analysis is not enough to identify it, this is due to the fact that it is periodic in a global sense and not separately on two directions like Lissajous orbits.

By exploiting the symmetry of the dynamical model the Halo orbit can be obtained by solving iteratively an orbit identification problem with the proposed initial guess. The correction on the initial guess is obtained through the State Transition Matrix which directly correlates variation of the initial state to the new final state.

The STM matrix is not obtainable in an analytical way for this problem, it was then decided to develop a first order approximation through forward finite differences with a step equal to $\boldsymbol{\varepsilon}_i = \sqrt{\epsilon}\, max(1, |\mathbf{x}_i|)$. Considering the flow of the problem $\boldsymbol{\varphi}(\mathbf{x}_1, t_1, t)$ the i-th column of the STM has the form in Eq. (4)

$$\Phi_i = \frac{\boldsymbol{\varphi}(\mathbf{x}_0 + \boldsymbol{\varepsilon}_i, t_0, t) - \boldsymbol{\varphi}(\mathbf{x}_0, t_0, t)}{\boldsymbol{\varepsilon}_i} \tag{4}$$

This iterative scheme will compute a final point by integrating the dynamical model until the condition $y = 0$ is met. It will then use Eq. (5a) by imposing that the new final state must have $v_x = 0$ and $v_z = 0$ and considering that the initial variables free to change are x_0 and v_y as shown in Eq. (5b).

$$\boldsymbol{x}_f^{new} = \boldsymbol{x}_f^{prev} + \boldsymbol{\Phi}\delta\boldsymbol{x}_0 \tag{5a}$$

$$\begin{bmatrix} \delta x^0 \\ \delta v_y^0 \end{bmatrix} = -\begin{bmatrix} \Phi_{41} & \Phi_{45} \\ \Phi_{61} & \Phi_{65} \end{bmatrix}^{-1} \begin{bmatrix} v_x^{prev} \\ v_z^{prev} \end{bmatrix} \tag{5b}$$

The initial state for the periodic orbit is $\mathbf{x}_0 = [1.00825,\ 0,\ 0.00121429,\ 0,\ 0.0103365,\ 0]$, while the trajectory is shown in Fig. 1.

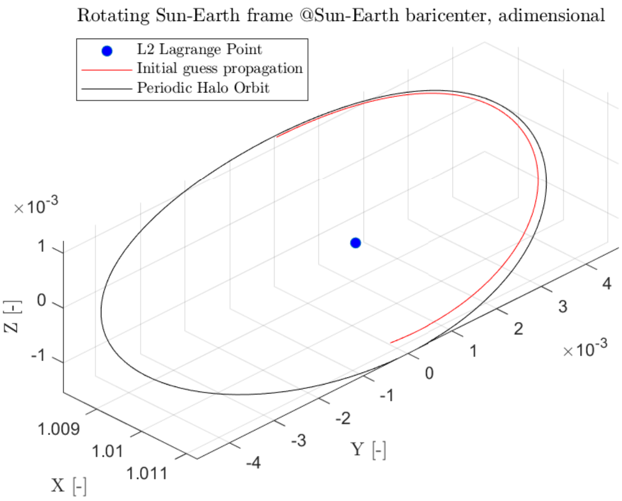

Figure 1: Guess and Solution Halo orbits

Considering the numerical continuation approach is important to choose an adequate size for the step between a z_0 and the next, to assure convergence of the process, a number of 10 orbits with a step of 3.4E-4 is found appropriate, the result is the orbit family in Fig. 2.

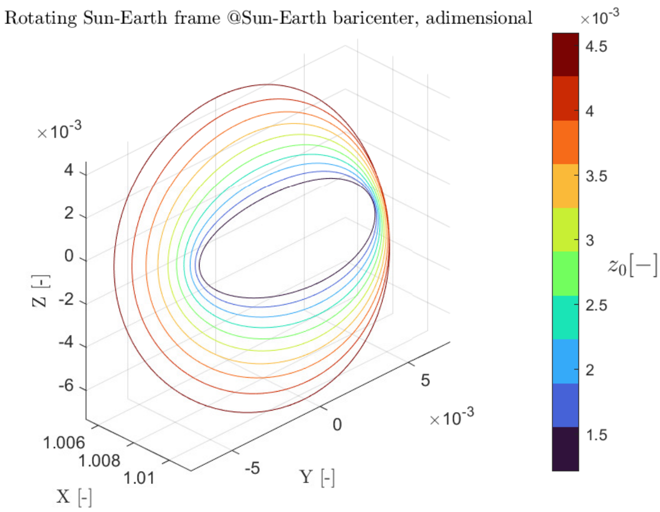

Figure 2: Halo orbit family

2 Impulsive guidance

Exercise 2

Consider the two-impulse transfer problem stated in Section 3.1 (Topputo, 2013)*.

1) Using the procedure in Section 3.2, produce a first guess solution using $\alpha = 1.5\pi$, $\beta = 1.41$, $\delta = 7$, and $t_i = 0$. Plot the solution in both the rotating frame and Earth-centered inertial frame (see Appendix 1 in (Topputo, 2013)).

2) Considering the first guess in 1) and using $\{\mathbf{x}_i, t_i, t_f\}$ as variables, solve the problem in Section 3.1 with simple shooting in the following cases

   a) without providing any derivative to the solver, and

   b) by providing the derivatives and by estimating the state transition matrix with variational equations.

3) Considering the first guess solution in 1) and the procedure in Section 3.3, solve the problem with multiple shooting taking $N = 4$ and using the variational equation to compute the Jacobian of the nonlinear equality constraints.

(11 points)

The objective of this work is to find an optimal two impulse maneuver in the Earth-Moon system with a PBRFBP dynamical model. The initial guess is displayed in Fig. 3a, from this figure it can be understood that this starting trajectory is relatively poor, then this local minima could be greatly improved with more optimization rounds or a grid search. A plot in the inertial frame is also displayed in Fig. 3b.

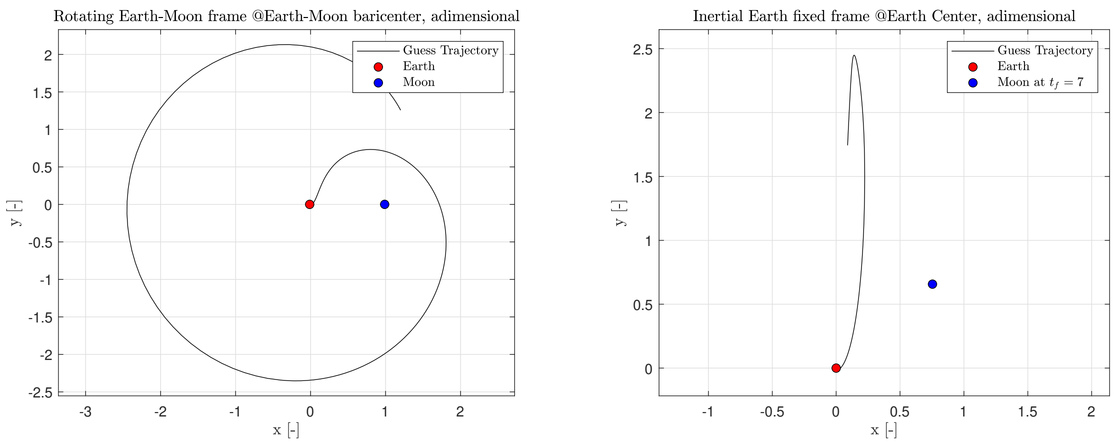

(a) Rotating Frame

(b) Inertial frame

Figure 3

Initially the problem is framed as a simple shooting, the state of the NLP is $\mathbf{x} = [\mathbf{x}_1\ , t_1,\ t_2]$. Then an objective function, which consist of the cost of two maneuvers tangents to the initial and final circular orbits around the targets, is defined in Eq. (6).

$$\Delta V_1 = \sqrt{(\dot{x}_i - y_i)^2 + (\dot{y}_i + x_i + \mu)^2} - \sqrt{\frac{(1-\mu)}{r_i}} \tag{6a}$$

*F. Topputo, "On optimal two-impulse Earth–Moon transfers in a four-body model", Celestial Mechanics and Dynamical Astronomy, Vol. 117, pp. 279–313, 2013, DOI: 10.1007/s10569-013-9513-8.

$$\Delta V_2 = \sqrt{(\dot{x}_f - y_f)^2 + (\dot{y}_f + x_f + \mu - 1)^2} - \sqrt{\frac{\mu}{r_f}} \tag{6b}$$

$$\Delta V = \Delta V_1 + \Delta V_2 \tag{6c}$$

The constraints impose that the final and initial points must be on the circular orbits respectively around Earth and the Moon, they are reported in Eq. (7) and Eq. (8). These are implemented as separate local Matlab functions and solved with fmincon. The functions optionally compute the gradient of the objective function and the Jacobian of the constraints, through a State Transition Matrix computed with the variational approach.

$$\mathbf{\Psi}_i = \begin{cases} (x_i + \mu)^2 + y_i^2 - r_i^2 = 0 \\ (x_i + \mu)(\dot{x}_i - y_i) + y_i(\dot{y}_i + x_i + \mu) = 0 \end{cases} \tag{7}$$

$$\mathbf{\Psi}_f = \begin{cases} (x_f + \mu - 1)^2 + y_f^2 - r_f^2 = 0 \\ (x_f + \mu - 1)(\dot{x}_f - y_f) + y_f(\dot{y}_f + x_f + \mu - 1) = 0 \end{cases} \tag{8}$$

By providing the analytical form of the derivatives it is expected a faster convergence with less iterations with respect to the use of finite difference approximations. These derivatives are reported in appendix A.

To optimize the search of the solution the functions can be defined as nested of a main function with a shared global state, then these procedures can avoid unnecessary computations by checking if the state has been updated or not. This optimization lead to a decrement of computation time of 49.25% and 62.4% with the derivatives. The results are contained in Table 2, while Fig. 4 shows at a glance the convergence of the method.

Method	Iteration	F-count	ΔV	Max Violation
No Derivatives	51	480	4.21488	5.333E-08
Derivatives	15	34	4.21838	6.296E-08

Table 2: Simple Shooting Results

To improve the robustness of the algorithm a multiple shooting method is implemented. The solution is defined with multiple arcs, the states of their start and end points are used as optimization variables and serve as beacons to guide the solution through various points along the path and avoid accumulation of integration errors. The statement of the problem is reported in Eq. (9) where the NLP state is $[\mathbf{x}_1 \ \cdots \ \ \mathbf{x}_n \ t_1 \ t_n]$.

$$\min \Delta V = \Delta V_1 + \Delta V_2 \tag{9a}$$

$$\text{subject to :} \quad \boldsymbol{\zeta}_k = \boldsymbol{\varphi}(\mathbf{x}_k, t_k, t_{k+1}) - \mathbf{x}_{k+1} = 0; \mathrm{k} = 1, \ \cdots, \mathrm{N} - 1 \tag{9b}$$

$$\text{subject to :} \quad \mathbf{\Psi}_i(\mathbf{x}_i, t_i) = 0, \quad \mathbf{\Psi}_f(\mathbf{x}_f, t_f) = 0 \tag{9c}$$

Inequalities to avoid impact with the main bodies and time reversal are also defined in Eq. (10)

$$\begin{cases} R_e^2 - (x_j + \mu)^2 + y_j^2 < 0, \\ R_m^2 - (x_j + \mu - 1)^2 + y_j^2 < 0, \quad \mathrm{j} = 1, \ \cdots, \mathrm{N}. \\ t_1 - t_N < 0 \end{cases} \tag{10}$$

The function was implemented general enough to decide the number of points on the trajectory to be used in the optimization, the results for various N are shown in Table 3, and in Fig. 5

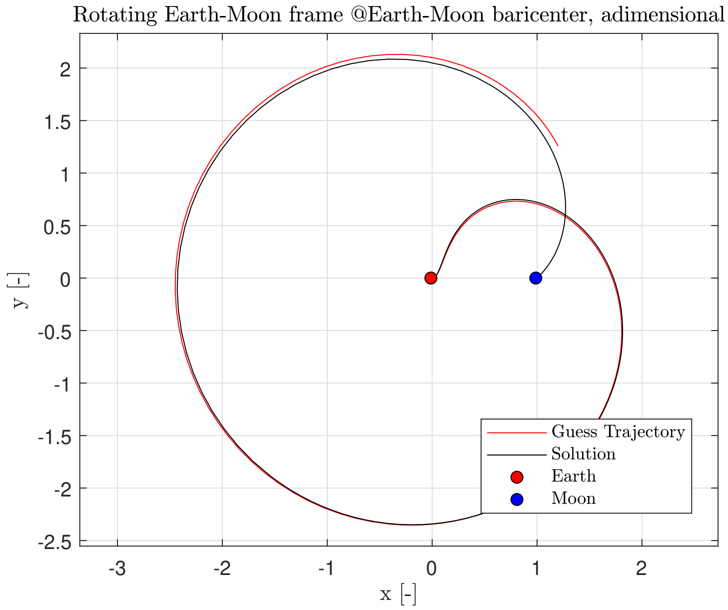

Figure 4: Guess and Solution Simple Shooting

Nodes number	Iteration	F-count	ΔV	Max Violation
N = 4	21	58	4.11265	1.344E-10
N = 10	31	116	4.24625	3.276E-08
N = 20	61	278	4.05091	4.975E-07

Table 3: Multiple Shooting Results

The gradient of the objective function, the Jacobian of the equality and inequality constraint for the multiple shooting method are reported in appendix B, the implementation uses sparse matrices for these mostly empty data in order to save space in the cases where the number of nodes is higher.

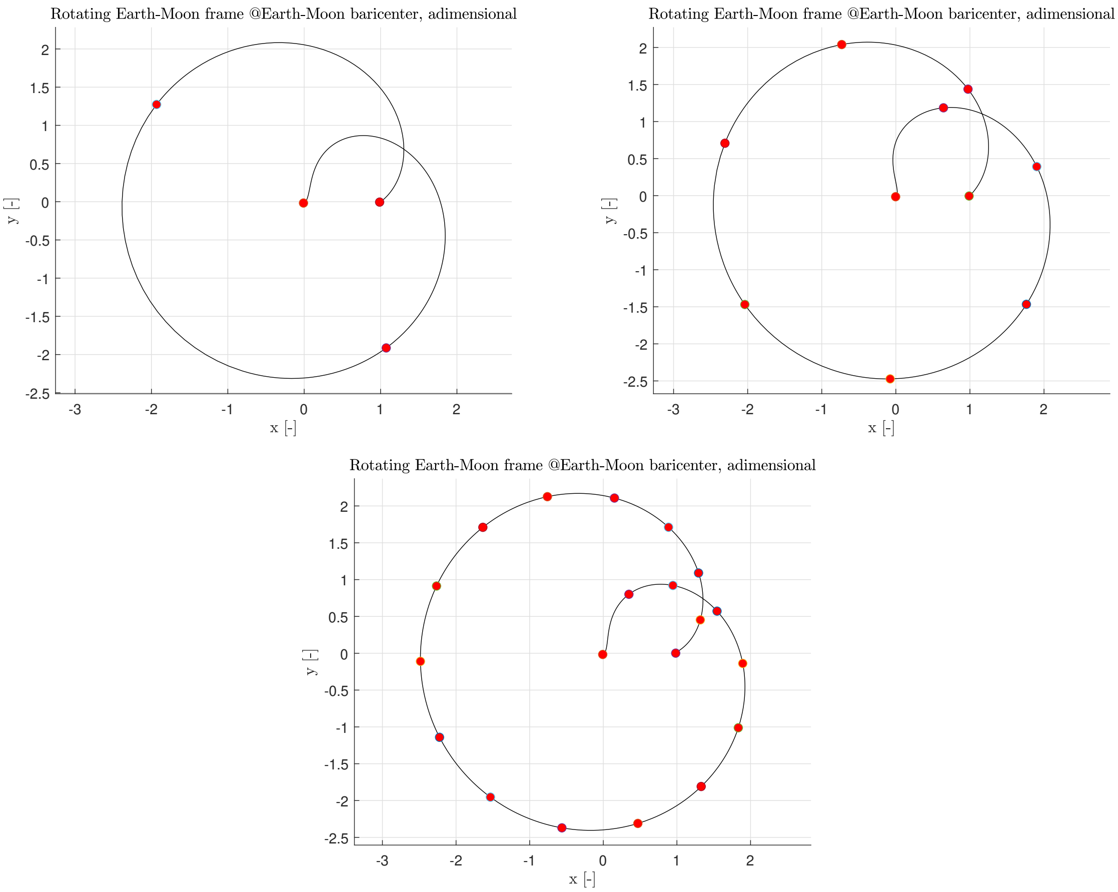

Figure 5: Solutions for various number of nodes N = 4, 10, 20

3 Continuous guidance

Exercise 3

A low-thrust option is being considered for an Earth-Mars transfer†. Provide a *time-optimal* solution under the following assumptions: the spacecraft moves in the heliocentric two-body problem, Mars instantaneous acceleration is determined only by the Sun's gravitational attraction, the departure date is fixed, and the spacecraft initial and final states are coincident with those of the Earth and Mars, respectively.

1) Write down the spacecraft equations of motion, the costate dynamics, and the zero-finding problem for the unknowns $\{\boldsymbol{\lambda}_0, t_f\}$ with the appropriate transversality condition.

2) Solve the problem considering the following data:

   – Launch date: `2022-08-03-12:45:20.000 UTC`
   – Spacecraft mass: $m_0 = 1500$ kg
   – Electric properties: $T_{\max} = 150$ mN, $I_{sp} = 3000$ s
   – Number of thrusters: 4

   Report the obtained solution in terms of $\{\boldsymbol{\lambda}_0, t_f\}$ and the error with respect to the target. Validate your results exploiting the properties of time-optimal solutions.

3) Solve the problem for a degraded configuration with only 3 thrusters available, assuming that the failure occurs immediately after launch. Plot the thrust angles and compare them to the nominal case in 2).

(11 points)

The problem is defined in a heliocentric two-body problem, the equations of motion are the ones reported in Eq. (11), the continuous propulsion is accounted for in the additional acceleration term and in the differential form of the rocket equation. The thrust is defined as $\mathbf{T} = T_{max} u \boldsymbol{\alpha}$ where T_{max} is the maximum available thrust, u identifies the level of thrust and $\boldsymbol{\alpha}$ the thrust direction.

$$
\begin{cases}
\dot{\mathbf{r}} = \mathbf{v} \\
\dot{\mathbf{v}} = -\dfrac{\mu}{r^3}\mathbf{r} - \dfrac{T_{max}}{m} u \boldsymbol{\alpha} \\
\dot{m} = -\dfrac{T_{max}}{I_{sp} g_0} u
\end{cases}
\tag{11}
$$

Then the costate-dynamics is derived from the Euler-Lagrange equations, in Hamiltonian form $\dot{\boldsymbol{\lambda}} = -\partial H / \partial \mathbf{x}$, and reported in Eq. (12)

$$
\begin{cases}
\dot{\boldsymbol{\lambda}}_r = -\dfrac{3\mu}{r^5}(\mathbf{r} \cdot \boldsymbol{\lambda}_v)\mathbf{r} + \dfrac{\mu}{r^3}\boldsymbol{\lambda}_v \\
\dot{\boldsymbol{\lambda}}_v = -\boldsymbol{\lambda}_r \\
\dot{\lambda}_m = -u \dfrac{\lambda_v T_{max}}{m^2}
\end{cases}
\tag{12}
$$

Using Pontryagin minimum principle which in a short form replaces $\partial H / \partial \mathbf{u} = 0$ with $\mathbf{u} = \operatorname{argmin} H(\mathbf{x}, \boldsymbol{\lambda}, \mathbf{u})$, the result is a actuation law with $\boldsymbol{\alpha} = -\boldsymbol{\lambda_v}/\lambda_v$ and u equal to 0 or 1 depending on the switch function $-(\lambda_v I_{sp} g_0)/m - \lambda_m$

†Read the necessary gravitational constants and planets positions from SPICE. Use the kernels provided on WeBeep for this assignment.

The problem has conditions both at the beginning and at the end of the integration, the method of solution in this case is the shooting method, in particular by guessing the initial costate and time of arrival the equations can be integrated directly, then the final state is checked for compatibility with the final condition, if the error on these is low enough the solution is accepted, otherwise the process must be repeated, to achieve the correctness of the final conditions the zero finding problem in Eq. (13) is implemented. The 4^{th} equation is the transversality condition which impose the Hamiltonian at the end of the leg, to have a specific value.

$$\begin{cases} \mathbf{r}(t_f) - \mathbf{r}_M(t_f) = 0 \\ \mathbf{v}(t_f) - \mathbf{v}_M(t_f) = 0 \\ \lambda_m(t_f) = 0 \\ H(t_f) - \boldsymbol{\lambda}_r \cdot \mathbf{v}_M(t_f) - \boldsymbol{\lambda}_v \cdot \mathbf{a}_M(t_f) = 0 \end{cases} \tag{13}$$

Because the various conditions involve variables expressed in units which can take different order of magnitudes the search with the triplet km, s, kg will be difficult. For the implementation an alternative set of units is chosen such as AU for space, Julian years for time and kg for mass. The implementation used the Matlab solver fsolve and a while loop with random generated guesses. The range in which the random guesses $[\boldsymbol{\lambda}_0, t_f]$ are generated was obtained by inspection of the dynamics by integrating multiple inputs.

The result in the nominal case (4 thrusters) is contained in Table 4, and in Table 5.

$\boldsymbol{\lambda}_{0,r}$	-4.04036	2.91114	0.200558
$\boldsymbol{\lambda}_{0,v}$	-0.826552	-0.385115	-0.0106874
$\lambda_{0,m}$	0.000477		
t_f	`2023-05-12-08:42:14.726 UTC`		
TOF [days]	281.8311		

Table 4: Time-optimal Earth-Mars transfer solution,4 thrusters.

$\|\|\mathbf{r}_f(t_f) - \mathbf{r}_M(t_f)\|\|$	[km]	0.00083364617
$\|\|\mathbf{v}_f(t_f) - \mathbf{v}_M(t_f)\|\|$	[m/s]	0.00000023276

Table 5: Final state error with respect to Mars' center, 4 thrusters.

The results are validated by the knowledge that for a time optimal problem the switch function is always less than 0. This means that the thrust is always on, and u maintains a constant value equal to 1. An ulterior validation comes from the exploitation of the Hamiltonian property $dH/dt = \partial H/\partial t = 0$, since both the integrated function in the objective and the vector field are constant, the Hamiltonian is kept constant. These results are reported in appendix C, to avoid cluttering of the main work.

By solving again in the case where the number of thrusters is reduced to 3 due to a malfunction the solutions are reported in Table 6, and in Table 7.

$\boldsymbol{\lambda}_{0,r}$	-11.4406	9.46747	0.156423
$\boldsymbol{\lambda}_{0,v}$	-2.37511	-1.25128	0.0182548
$\lambda_{0,m}$	0.001186		
t_f	`2023-10-16-03:55:14.519 UTC`		
TOF [days]	438.6319		

Table 6: Time-optimal Earth-Mars transfer solution.

$\|\|\mathbf{r}_f(t_f) - \mathbf{r}_M(t_f)\|\|$	[km]	0.17074426560
$\|\|\mathbf{v}_f(t_f) - \mathbf{v}_M(t_f)\|\|$	[m/s]	0.00002151376

Table 7: Final state error with respect to Mars' center.

These outcomes show that a loss of a thruster requires around 5 more months to complete, a longer transfer time could violate mission requirements, such as maximum storable propellant, the extra consumption infact require 83 kg more than the nominal case, or maximum propellant storage time, so the feasibility of this case depends on the particular mission. The errors in the final position and velocity are greater, but are still acceptable.

The definition of the thrust angles is displayed in Fig. 6, since the computation are done in an ecliptic J2000 frame then the x axis is the vernal equinox axis while the z axis is the normal to the ecliptic plane. The in plane angle is named Azimuth, it is the angle with respect to the γ line, positive clockwise. The out of plane angle is named Elevation, it is the angle with respect to the projection of the vector on the ecliptic plane, greater than zero for vectors with positive z coordinates.

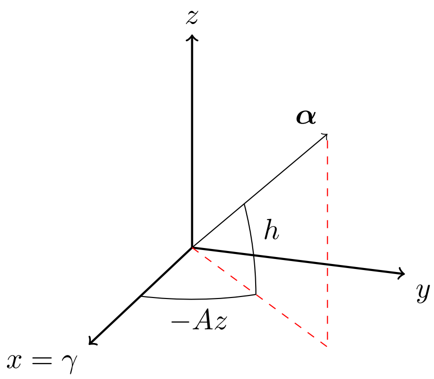

Figure 6: Definition of the thrust angles.

The thrust angles for the two cases are displayed in Fig. 7a and Fig. 7b.

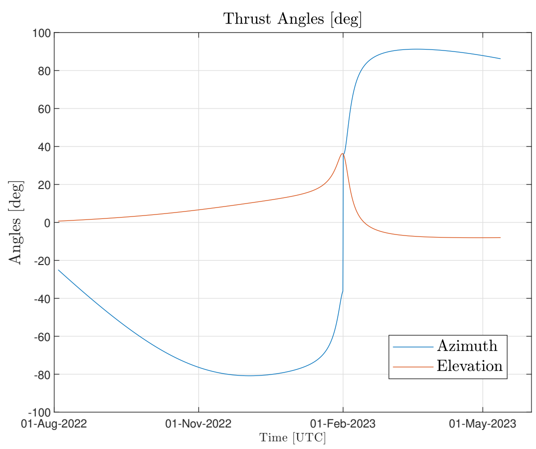

(a) Four Thrusters

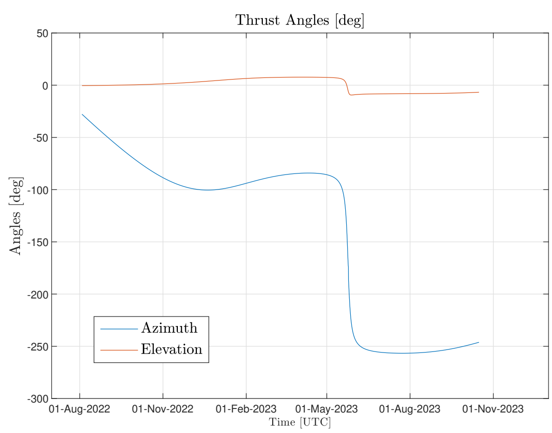

(b) Three Thrusters

Figure 7: Plot of thrust angles for the two cases.

In Fig. 10a and Fig. 10b it is visible the in plane thrust direction during the orbit. In both the cases the thrust has a relatively quick change of angle in the middle of the trajectory. In general it can be said that the elevation thrust angle remain small since the initial Earth orbit and Mars orbit are almost on the same plane. The Azimuth angle on the other hand will change significantly and can be though as having 2 phases: in the first the thrust direction is towards the target orbit, then a switch happens which pass through a tangent condition with respect to the spacecraft velocity and into a second phase where the Azimuth angle is almost constant.

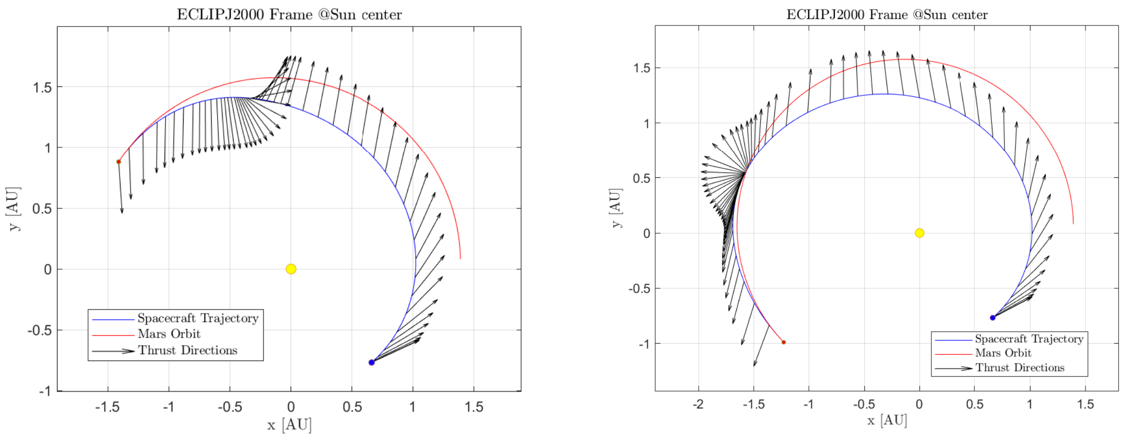

(a) Four Thrusters

(b) Three Thrusters

Figure 8: Plot of in-plane thrust direction for the two cases

Appendices

A Derivatives of Simple Shooting

This appendix section reports the derivatives of the simple shooting method. First the derivatives that compose the gradient are shown in Eq. (14).

$$\frac{d\Delta V_1}{d\mathbf{x}_i} = \frac{1}{\sqrt{(\dot{x}_i - y_i)^2 + (\dot{y}_i + x_i + \mu)^2}} \begin{bmatrix} \dot{y}_i + x_i + \mu \\ y_i - \dot{x}_i \\ \dot{x}_i - y_i \\ \dot{y}_i + x_i + \mu \end{bmatrix} \tag{14a}$$

$$\frac{d\Delta V_2}{d\mathbf{x}_f} = \frac{1}{\sqrt{(\dot{x}_f - y_f)^2 + (\dot{y}_f + x_f + \mu - 1)^2}} \begin{bmatrix} \dot{y}_f + x_f + \mu - 1 \\ y_f - \dot{x}_f \\ \dot{x}_f - y_f \\ \dot{y}_f + x_f + \mu - 1 \end{bmatrix} \tag{14b}$$

$$\frac{d\Delta V_2}{d\mathbf{x}_i} = \frac{d\Delta V_2}{d\mathbf{x}_f}\Phi \qquad \frac{d\Delta V}{d\mathbf{x}_i} = \frac{d\Delta V_1}{d\mathbf{x}_i} + \frac{d\Delta V_2}{d\mathbf{x}_i} \tag{14c}$$

$$\frac{d\Delta V}{dt_1} = \frac{d\Delta V_2}{d\mathbf{x}_f}\mathbf{f}(\mathbf{x}(t_2), t_2) \qquad \frac{d\Delta V}{dt_2} = -\frac{d\Delta V_2}{d\mathbf{x}_f}(\Phi\mathbf{f}(\mathbf{x}_i, t_i)) \tag{14d}$$

The derivatives of the equality constraint which compose the Jacobian are displayed in Eq. (15)

$$\frac{d\mathbf{c}_i}{d\mathbf{x}_i} = \begin{bmatrix} 2\mu + 2x_i & 2y_i & 0 & 0 \\ \dot{x}_i & \dot{y}_i & \mu + x_i & y_i \end{bmatrix} \tag{15a}$$

$$\frac{d\mathbf{c}_f}{d\mathbf{x}_f} = \begin{bmatrix} 2(\mu + x_f - 1) & 2y_f & 0 & 0 \\ \dot{x}_f & \dot{y}_f & \mu + x_f - 1 & y_f \end{bmatrix} \tag{15b}$$

$$\frac{d\mathbf{c}_f}{d\mathbf{x}_i} = \frac{d\mathbf{c}_f}{d\mathbf{x}_f}\Phi \tag{15c}$$

$$\frac{d\mathbf{c}_f}{dt_i} = -\frac{d\mathbf{c}_f}{d\mathbf{x}_f}\Phi\mathbf{f}(x_i, t_i) \tag{15d}$$

$$\frac{d\mathbf{c}_f}{dt_f} = \frac{d\mathbf{c}_f}{d\mathbf{x}_f}\mathbf{f}(\mathbf{x}_f, t_f) \tag{15e}$$

B Derivatives of Multiple Shooting

This appendix section reports the derivatives of the multiple shooting method. First the derivatives that compose the gradient are shown in Eq. (16).

$$\frac{d\Delta V}{d\mathbf{x}_i} = \frac{1}{\sqrt{(\dot{x}_i - y_i)^2 + (\dot{y}_i + x_i + \mu)^2}} \begin{bmatrix} \dot{y}_i + x_i + \mu \\ y_i - \dot{x}_i \\ \dot{x}_i - y_i \\ \dot{y}_i + x_i + \mu \end{bmatrix} \tag{16a}$$

$$\frac{d\Delta V}{d\mathbf{x}_f} = \frac{1}{\sqrt{(\dot{x}_f - y_f)^2 + (\dot{y}_f + x_f + \mu - 1)^2}} \begin{bmatrix} \dot{y}_f + x_f + \mu - 1 \\ y_f - \dot{x}_f \\ \dot{x}_f - y_f \\ \dot{y}_f + x_f + \mu - 1 \end{bmatrix} \tag{16b}$$

$$\nabla f = \begin{bmatrix} \frac{d\Delta V}{d\mathbf{x}_i} & 0 & \cdots & 0 & \frac{d\Delta V}{d\mathbf{x}_f} & 0 & 0 \end{bmatrix} \tag{16c}$$

The derivatives of the equality constraints which link one arc to another are displayed in Eq. (17)

$$\frac{d\boldsymbol{\zeta}_k}{d\boldsymbol{\zeta}_k} = \Phi(t_k, t_{k+1}) \quad \frac{d\boldsymbol{\zeta}_k}{d\mathbf{x}_{k+1}} = -\mathbf{I}_{6x6} \quad \mathrm{k} = 1, ..., \mathrm{n} - 1 \tag{17a}$$

$$\begin{aligned} \frac{d\boldsymbol{\zeta}_k}{dt_1} &= \frac{dt_k}{dt_1}\frac{d\boldsymbol{\varphi}}{dt_k} + \frac{dt_{k+1}}{dt_1}\frac{d\boldsymbol{\varphi}}{dt_{k+1}} = -\frac{m-k}{m-1}\Phi(t_k, t_{k+1})\mathbf{f}(\mathbf{x}_k, t_k) \\ &+ \frac{m-k-1}{m-1}\mathbf{f}(\boldsymbol{\varphi}(\mathbf{x}_k, t_k, t_{k+1}), t_{k+1})) \quad \mathrm{k} = 1, ..., \mathrm{n} \end{aligned} \tag{17b}$$

$$\begin{aligned} \frac{d\boldsymbol{\zeta}_k}{dt_m} &= \frac{dt_k}{dt_m}\frac{d\boldsymbol{\varphi}}{dt_k} + \frac{dt_{k+1}}{dt_m}\frac{d\boldsymbol{\varphi}}{dt_{k+1}} = -\frac{k-1}{m-1}\Phi(t_k, t_{k+1})\mathbf{f}(\mathbf{x}_k, t_k) \\ &+ \frac{k}{m-1}\mathbf{f}(\boldsymbol{\varphi}(\mathbf{x}_k, t_k, t_{k+1}), t_{k+1})) \quad \mathrm{k} = 1, ..., \mathrm{n} \end{aligned} \tag{17c}$$

The derivatives of the equality constraints which constrain the final and initial state are displayed in Eq. (18)

$$\frac{d\Psi_i}{d\mathbf{x}_i} = \begin{bmatrix} 2\mu + 2x_i & 2y_i & 0 & 0 \\ \dot{x}_i & \dot{y}_i & \mu + x_i & y_i \end{bmatrix} \tag{18a}$$

$$\frac{d\Psi_f}{d\mathbf{x}_f} = \begin{bmatrix} 2(\mu + x_f - 1) & 2y_f & 0 & 0 \\ \dot{x}_f & \dot{y}_f & \mu + x_f - 1 & y_f \end{bmatrix} \tag{18b}$$

At last the derivatives of the inequality constraints are reported in Eq. (19)

$$\frac{d\mathbf{c}_j}{d\mathbf{x}_j} = \begin{bmatrix} -2\mu - 2x_j & -2y_j \\ -2(x_j + \mu - 1) & -2y_j \end{bmatrix} \quad \mathrm{j} = 1, ..., \mathrm{n} \tag{19}$$

C Visual Results of Continuous Thrust

In this appendix are reported the thrust levels as validation of the time optimal control and other representative graphs of the correctness of the transfers.

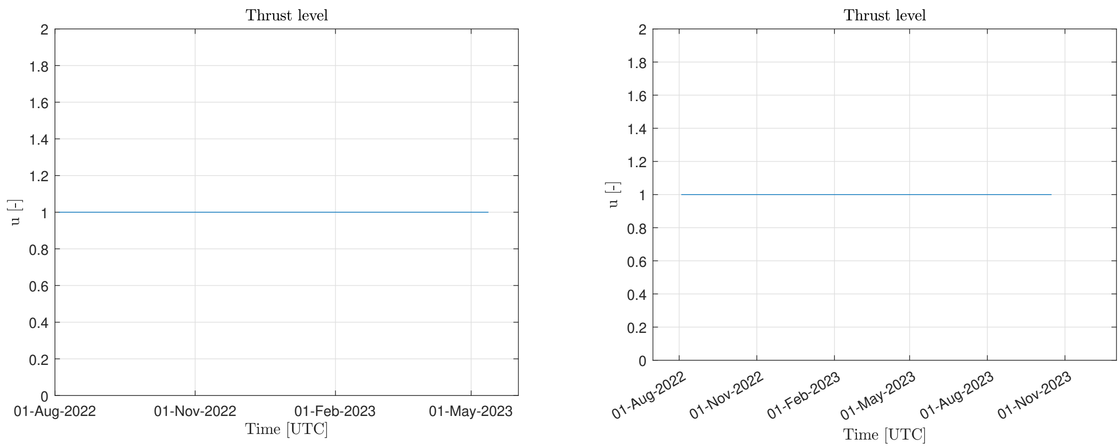

(a) Four Thrusters **(b)** Three Thrusters

Figure 9: Thrust levels for the two cases

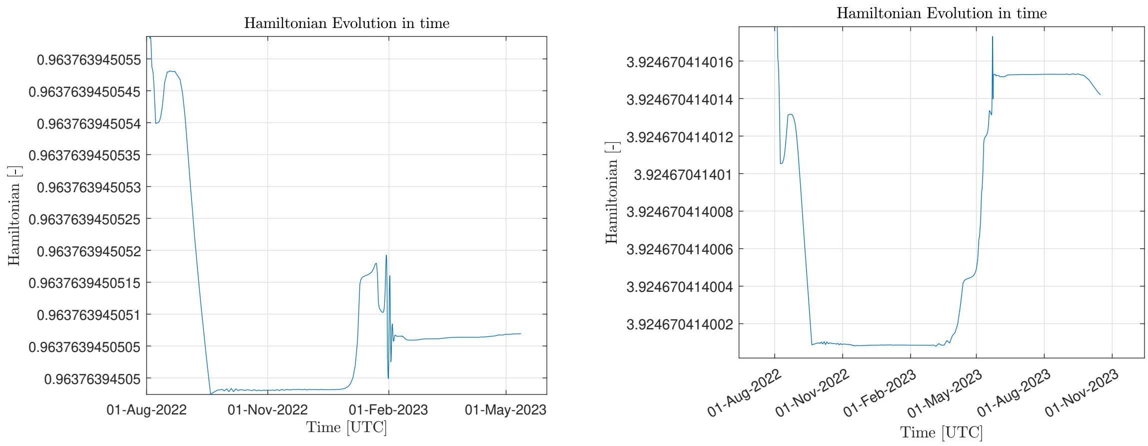

(a) Four Thrusters **(b)** Three Thrusters

Figure 10: Hamiltonian for the two cases